Journal of Hazardous Materials 213–214 (2012) 161–166

Contents lists available at SciVerse ScienceDirect

Journal of Hazardous Materials

journal homepage: www.elsevier.com/locate/jhazmat

Green synthesis of nanosilver as a sensor for detection of hydrogen peroxide in water

Vineet K. Shukla[a,b,*], Raghvendra S. Yadav[a], Poonam Yadav[c], Avinash C. Pandey[a]

[a] Nanotechnology Application Centre, Faculty of Science, University of Allahabad, Allahabad 211002, India
[b] Department of Physics, Faculty of Science, University of Allahabad, Allahabad 211002, India
[c] National Physical Laboratory, Dr. K. S. Krishnan Marg, New Delhi 110012, India

ARTICLE INFO

Article history:
Received 23 September 2011
Received in revised form 3 December 2011
Accepted 22 January 2012
Available online 4 February 2012

Keywords:
Green synthesis
Nanosilver
Hydrogen peroxide
Electro-catalysis
Sensors
FTIR

ABSTRACT

Present "green" synthesis is an efficient, easy-going, fast, renewable, inexpensive, eco-friendly and non-toxic approach for nanosilver formation, which offers numerous benefits over physiochemical approaches. The X-ray diffraction (XRD) pattern suggests the formation and crystallinity of nanosilver. The average particle size of silver nanoparticles was 8.25 ± 1.37 nm as confirmed by transmission electron microscopy (TEM). The UV–vis absorption spectrum shows a characteristic absorption peak of silver nanoparticles at 410 nm. FTIR confirms Azadirachtin as reducing and stabilizing agent for nanosilver formation. In addition, the nanosilver modified electrode (Ag/GC) exhibited an excellent electro-catalytic activity toward the reduction of hydrogen peroxide (H_2O_2). The produced nanosilver is stable and comparable in size. These silver nanoparticles show potential applications in the field of sensors, catalysis, fuel cells and nanodevices.

1. Introduction

Nanosilver (NS) magnetizes a significant awareness because of its wide range of applications in emerging areas of nanoscience and technology [1]. Size, shape, and surface morphology play pivotal roles in controlling the physical, chemical, optical, and electronic properties of these nanoscopic materials [2,3]. Over the past decade there has been an increased emphasis on the topic of "green" chemistry and processes. These efforts aim at the total elimination or at least the minimization of generated waste and the implementation of sustainable processes through the adoption of 12 fundamental principles [4–6]. Any attempt meeting these goals must comprehensively address these principles in the design of a synthesis routes, chemical analysis or chemical process [4,6]. Utilization of nontoxic chemicals; environmentally benign solvents and renewable materials are some of the key issues that merit important consideration in a green synthesis strategy [7]. The three main steps in the preparation of nanomaterials that should be evaluated from a green chemistry perspective are the choices of the solvent medium used for the synthesis, the choice of an environmentally benign reducing agent, and the choice of a nontoxic material for the stabilization of the nanoparticles [8]. The great deal of efforts has been established for green synthesis of inorganic materials, especially noble metal nanoparticles using microorganisms such as bacteria, actinomycetes and fungi [9–11]. The main drawback of this method is the need to purify the sample and extract because pathogenic bacteria might contaminate nanoparticles.

On other hand, the use of various parts of plants in similar nanoparticles synthesis can be potentially eliminate this problem by making the nanoparticles more bio-compatible and non-toxic, as it eliminates the elaborate process of maintaining the microbial culture and often found to be kinetically favorable than other bioprocesses. Jose-Yacaman and co-workers reported the formation of gold and silver nanoparticles using living plants. Recently silver nanoparticles have been synthesized using various plant products like green tea (*Camellia sinensis*), natural rubber, starch, aloe vera plant extract, lemongrass leaves extract leguminous shrub (*Sesbania drummondii*), latex of *Jatropha curcas*, neem leaf, etc. In this regard, Shankar et al. suggested that the reduction of aqueous $AuCl_4^-$ and Ag^+ ions using extracts from geranium and lemongrass plants were occur due to the ketones/aldehydes groups present in the extract which plays an important role in directing the shape evolution in these nanoparticles. Ankamwar et al. also synthesized gold nanotriangles using tamarind leaf extract as the reducing

* Corresponding author at: Nanotechnology Application Centre, Faculty of Science, University of Allahabad, Allahabad 211002, India. Tel.: +91 532 2460675; fax: +91 532 2460675.
E-mail address: vineet2shukla@gmail.com (V.K. Shukla).

0304-3894/$ – see front matter © 2012 Elsevier B.V. All rights reserved.
doi:10.1016/j.jhazmat.2012.01.071

agent and identified that tamarind plant as a potential candidate for shape-controlled synthesis of gold nanoparticles due to tartaric acid (—COOH) [10–18].

The current approach involves totally green approach for formation and stabilization of nanosilver via neem kernel extract at room temperature. There are many advantages of using neem kernel for silver nanoparticles formation. Firstly, neem kernel is quite commonly available, stored and used up to 3–8 months, requires only one-fourth than that of neem leaf extract and the main constituents Azadirachtin was present in higher extent than that of neem leaves. Secondly, it excludes addition of external stabilizing agent during synthesis, gives faster reaction kinetics, provide better stability, offers better control over shape and size with higher crystallinity. In present study, the number of carboxylate groups available in neem kernel extracts facilitates the complexion of silver ions to the molecular mold. Analogously, it is plausible that neem kernel extracts can play a significant role in reduction and stabilization of nanosilver. Furthermore, there are several key advantages to the use of this renewable material as the protecting agent. First, it is possible to form a dispersion of the neem kernel extract in H_2O, and so one can completely avoid the use of organic solvents. Second, the binding interaction between neem kernel extracts and the metal nanoparticles is comparatively weak as compared to the interaction between the nanoparticles and typical thiol-based protecting groups. This implies that the protection should be smoothly reversible at passably higher temperatures, enabling the separation of these particles. Additionally, it is possible that the use of place exchange reactions [19] could be used to comfortably functionalize the nanoparticles. Finally, and perhaps most importantly, neem kernel extract-protected nanosilver can be readily integrated into systems relevant for pharmaceutical and biomedical applications.

Some authors also reported silver nanoparticles formation using neem leaf [17,18] and many of researchers points out what is the differentia between silver nanoparticles obtained using neem leaf and neem kernel extract. As we know that in nanotechnology, the control over particles shape and size is a real challenge and it play very important role to control the applications. Moreover, we also want to increase the reaction kinetics as well as greater stability of nanoparticles. We performed the experiment in similar fashion as we have already done with the neem leaf extract but the results in both the cases are very different. Silver nanoparticles in case of neem leaf extract were agglomerated, poly-dispersed as well as particle size are in the range of 5–50 nm (wide range), takes 2–24 h to complete reaction kinetics and shows UV–vis absorption spectra near 450 nm. On the other hand, formation of silver nanoparticles using neem kernel extract takes only 20 min to complete reaction kinetics, show particles in the range of 6–14 nm with spherical shape and crystalline in nature with UV–vis spectra occurs at 410 nm. Hence, a blue-shift occurs indicating toward smaller size of silver nanoparticles formation. During our experiment we can find that greater extent of Azadirachtin increases the reaction kinetics as well as greater control over the shape and size of silver nanoparticles than by using the neem leaves. The main reason for this is the biochemical difference between the silver precipitating neem kernel extract and neem leaf extract is the overall charge of the Azadirachtin biomolecules which is greater in neem kernel extract. Hence the use of neem kernel extracts offers improvement in all the sections of silver nanoparticles formation.

2. Experimental details

In a typical method, 10 g neem kernel was washed thoroughly with distilled water and dried in the air. These neem kernels were crushed it into small pieces and boiled in 50 ml distilled water for 10 min. The cooled filtrate was adjusted at pH 10 by adding 1 M NaOH. Now, 1.0 ml of above prepared extract was added drop by drop in 100 ml of 10 mM $AgNO_3$ (Merck) in a conical flask. The above solution was placed on a magnetic stirrer for 20 min and centrifuged at 10,000 rpm for 10 min. The residue was washed several times with double distilled water followed by ethanol (Fig. 1). Finally, the residue was kept in the vacuum oven at 40 °C for drying. For electro catalytic oxidation, Glassy Carbon (GS) substrates were cleaned with distilled water several times and air dried. The reaction mixture well vortexes and the substrate were put inside it. A thin Ag film was formed on the GS substrate. This Ag/GS electrode was washed with the buffer solution and used in three electrodes cell as working electrode for electro catalytic activity. Its electro catalytic activity was compared with the pure GS electrode.

3. Characterization

UV–vis absorption spectroscopy was taken on Perkin Elmer model L35 spectrometer. XRD was performed on Rigaku D/max-2200 PC diffractometer operated at 40 kV/20 mA, using Cu $K\alpha_1$ radiation with wavelength of 1.54 Å. FTIR spectroscopy measurements were carried out on a NICOLET-5700 (Thermo Electron Corporation) in the range of 3500–500 cm^{-1}. Transmission electron microscopy (TEM) was done on Technai 30 G^2 S-Twin electron microscope operated at 300 kV accelerating voltage. Cyclic voltammetry (CV) was performed on an electrochemistry workstation CHI 660A (Austin, USA). These measurements were performed in a conventional three electrode electrochemical cell using Ag/GS and pure GS as the working electrode, platinum wire as the auxiliary electrode, and Ag/AgCl (saturated with KCl) as the reference electrode.

4. Results and discussion

UV–vis absorption spectroscopy is a main tool to analyze the noble metal nanoparticles formation, which depends on surface plasmon resonance (SPR). The localized SPR's are collective oscillations of the conduction electrons confined to metallic nanoparticles. Excitation of the localized surface plasmons causes strong light scattering by an electric field at a wavelength where resonance occurs; this phenomenon results in the appearance of strong SPR bands. The optical absorption spectrum of metal nanoparticles is dominated by the SPR, which depends upon the particle size, shape, state of aggregation and the surrounding dielectric medium [20]. When the extract is mixed in the $AgNO_3$ solution, the solution first becomes yellowish after 3 min and then finally brownish after reaction completion (20 min), indicating the formation of nanosilver [21]. The UV–vis absorption spectrum of the sample shows reaction kinetics of 20 min, showing the surface plasmon absorption of nanosilver at 410 nm (Fig. 2A). The formation of the nanosilver starts with the addition of the neem kernel extract which increases rapidly after 2 min and starts stabilization after 14 min. No change in peak was observed after 20 min, i.e., all silver ions were consumed within 20 min. Since, the last three spectra of 16, 18 and 20 min are overlapped on each other in Fig. 2A, because there are very minute differences in these three spectra. Therefore, re-plot of the peak points of these three spectra is shown in Fig. 2B, so that one can grasp the whole spectra, i.e., 11 spectra clearly.

XRD pattern of synthesized nanosilver shows face-centered-cubic (fcc) lattice (JCPDS file no. 04-0783) with strong diffraction peaks at 37, 44, 66 and 77 degrees of 2θ corresponds to (1 1 1), (2 0 0), (2 2 0) and (3 1 1) crystal planes (Fig. 3). The broadening of XRD peaks (i.e., Scherer's broadening) attributes nanosized

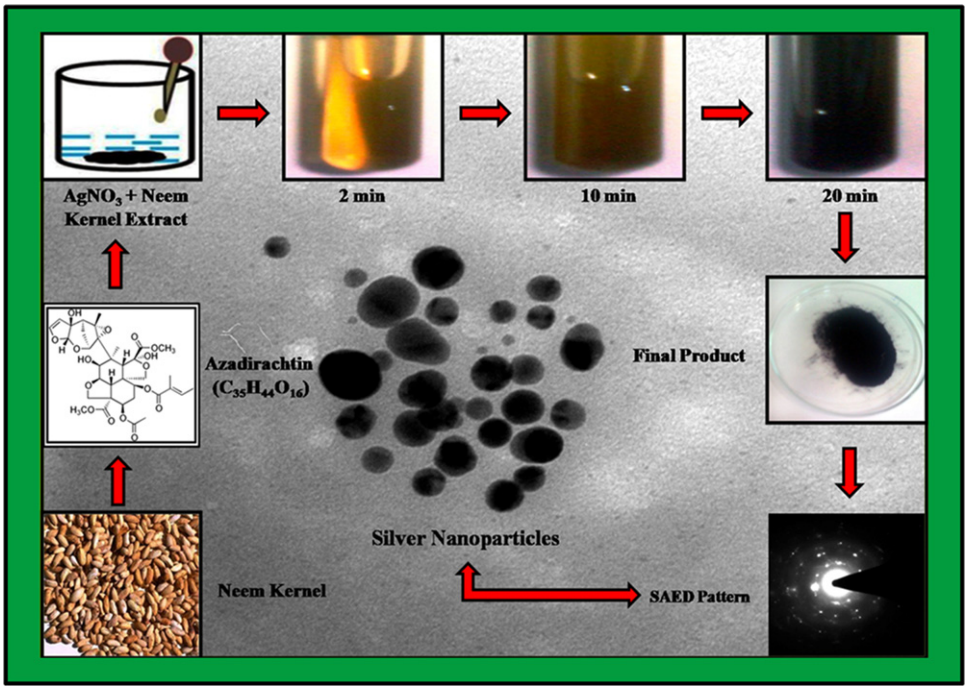

Fig. 1. Schematic graphic of nanosilver formation via neem kernel extract.

formation of silver nanocrystals. The crystallite sizes, d, of silver nanoparticles were estimated by Debye–Scherer's equation:

$$d = \frac{0.9\lambda}{\beta \cos\theta}$$

where d is the crystallite size, λ is the wavelength of radiation used, θ is the Bragg angle and β is the full width at half maxima (FWHM) on 2θ scale. Debye–Scherer's equation gives an average crystallite size of 5.5 ± 0.95 nm. No other diffraction peaks could be detected confirming phase-pure nanosilver formation.

FTIR spectroscopy was done to know the compound responsible for reduction and stabilization of nanosilver. For comparison, two drops of the neem kernel extract and two drops of the supernatant collected after centrifugation were mixed with KBr powder and palletized after drying properly. Over there is a slight change in the spectrum before (a) and after (b) reaction of the neem kernel extracts (Fig. 4), but both show the presence of bonds due to ester —C—O stretching (around 1740 cm^{-1}), carbonyl group —C=O (around 1651 cm^{-1}) and methyl group —C—H bending (around 1450 cm^{-1}). These bands are indicative of an Azadirachtin compound present in the aqueous neem kernel extract. *Azadirachtin* ($C_{35}H_{44}O_{16}$) is a chemical compound belongs to limonoids, which is a secondary metabolite of a neem kernel. *Azadirachtin* is a highly oxidized tetranortriterpenoid which boast a plethora of oxygen functionality, and it is compatible for nanoparticles formation and stabilization. Since, *Azadirachtin* had carboxylate ligands, and it

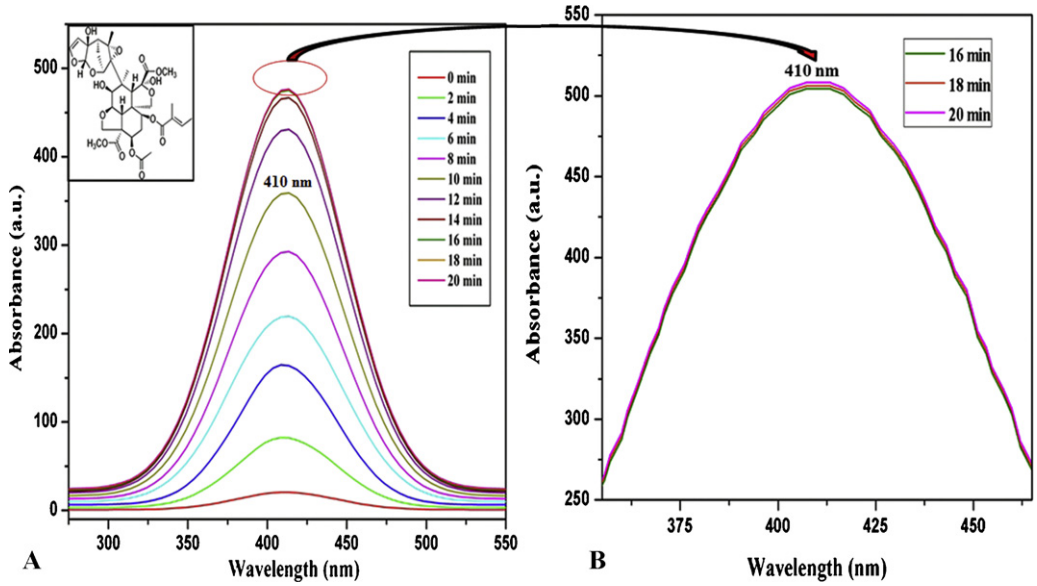

Fig. 2. (A) The surface plasmon absorbance spectrum of nanosilver formed in the neem kernel extract dispersion (λ_{max} = 410 nm). Inset shows *Azadirachtin* chemical structure. (B) The peak points of the last three spectra of 16, 18 and 20 min.

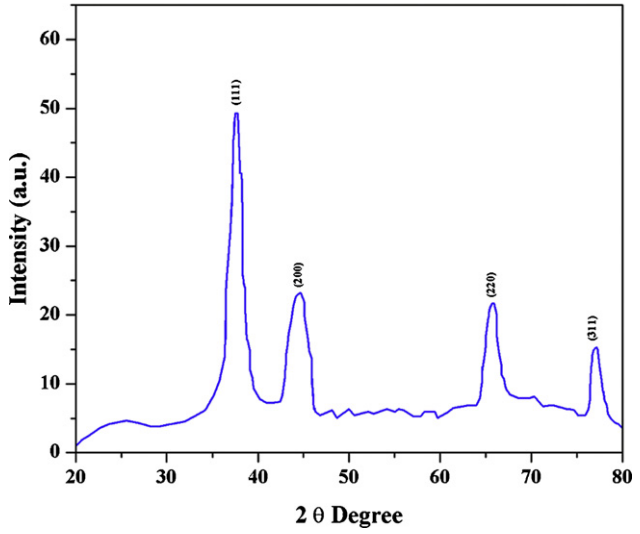

Fig. 3. The X-ray diffraction pattern of nanosilver having diffraction peaks at 37, 44, 66 and 77 degrees of 2θ.

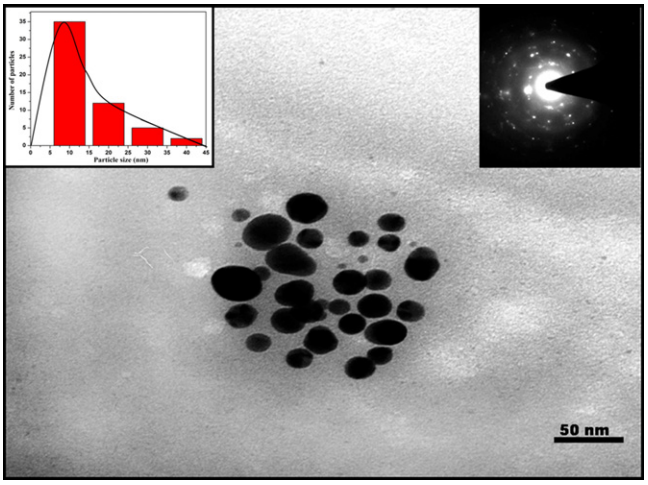

Fig. 5. TEM micrograph of synthesized nanosilver via neem kernel extract. The left inset show histogram of particle size distribution and the right inset show SAED pattern of synthesized nanosilver.

has a great ability to adopt different bonding modes, unidentate, bidentate, or bridging and therefore satisfied many metal's coordination preferences. Carboxylic anions (—COO^-) of *Azadirachtin* can covalently link to Ag, forming Ag-carboxylate (—COO–Ag) and the tails have hydrophobic and Vander Waals's interaction between hydrocarbon chains. Thus, the Ag^+ ions are then reduced by the *Azadirachtin* which acted as a strong reducing agent due to the presence of carboxyl groups leading to change in their secondary structure and the formation of Ag^0. These silver nuclei subsequently grew by the further reduction of silver ions and their accumulation of the nuclei. Therefore, formation of nanosilver has occurred.

A typical transmission electron microscope (TEM) image of the nanoparticles formed is presented in Fig. 4. In general, the particles are isotropic (i.e., the low aspect ratio) in shape. These results illustrate the synthesis of Ag^0 nanoparticles through reduction of Ag^+ inside the nanoscopic neem kernel extract templates. The carboxyl groups act as passivation contacts for the stabilization of the nanoparticles formed inside these templates. The left inset of Fig. 5 shows a histogram of the particle size distribution with the mean particle diameter 8.25 ± 1.37 nm. More than 65% of the nanosilver is in the size range from 6 to 14 nm, indicating the possible size selectivity of the neem kernel extract templates. The right inset of Fig. 5 shows the selective area electron diffraction (SAED) pattern containing a set of spots revealing high crystallinity of synthesized nanosilver. While these preliminary results demonstrate the proof of concept, it may be possible that better control of the particle size and crystallinity are achievable through the proper choice of the many reducing and stabilizing plant extracts available as well as minimization of environmental conditions. The solutions of dispersed nanosilver in neem kernel extract are highly stable and show no signs of aggregation even after three months of storage.

Cyclic voltammetry is one of the most common techniques used in electrochemistry to determine electro activity. Here, CVs of the pure GC electrode and GC electrode modified with Ag were measured in 0.1 M KH_2P0_4 solution at different scan rates (Fig. 6). The CVs of the pure GC shows a well-defined reversible redox process [22], whereas of Ag/GC shows a peak shift toward fewer positive and negative regions corresponding to anodic and cathodic potentials respectively. The Ag/GC electrode shows oxidation (1.05 V) and reduction (0.30 V) due to silver nanoparticles. When the scan rate is varied from 10 to 100 mV/s (from inside to outside corresponding to be $v = 10$, 20, 30, 40, 50, 60, 80, and 100 mV/s), the cathodic peak potentials are almost the same as the corresponding anodic

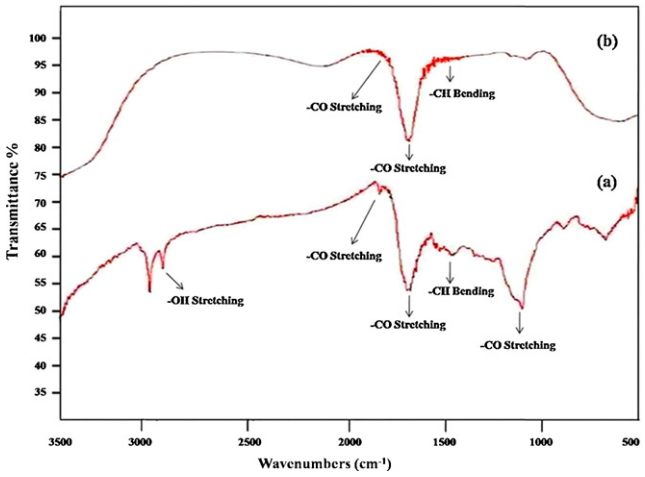

Fig. 4. FTIR spectrum of nanosilver before (a) and after (b) the reaction.

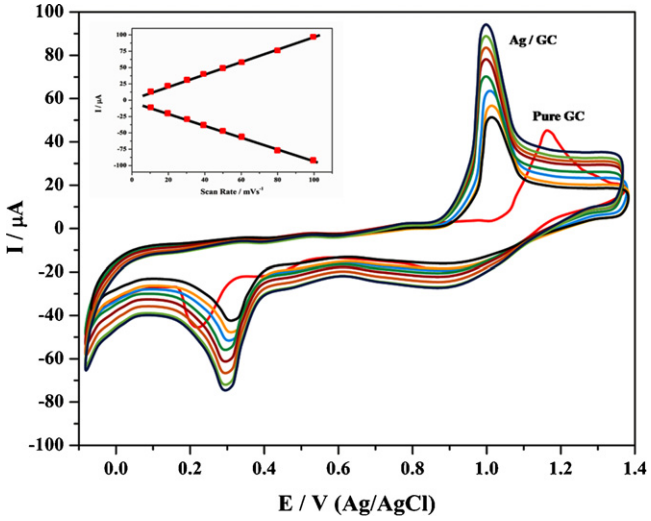

Fig. 6. CVs of pure GC and Ag/GC electrodes in 0.1 M KH_2P0_4 solution with different scan rates (from inner curve to outer curve: 10, 20, 30, 40, 50, 60, 80, and 100 mV/s, respectively). Insets show the relationship of the redox current of peak I and scan rate.

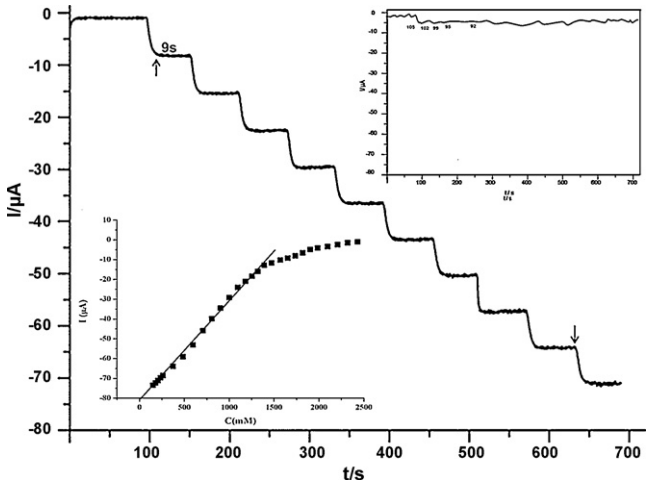

Fig. 7. The amperometric response of the sensor at −0.42 V to successive addition of 1.0 mM H_2O_2 to 0.2 M acetate buffer (pH 5). Left inset shows the calibration plot between the steady-state current and H_2O_2 concentration. Right inset shows the amperometric responses of two relevant electro active species (UA, AA, and 0.1 mM, respectively) and H_2O_2 (1.0 mM) on a modified Ag NS GC electrode at a working potential of −0.42 V.

peak potentials. The cathodic peak potentials shift to the negative direction, and the corresponding anodic peak potentials shift to the positive direction with increasing scan rate. The peak currents of the two redox couples increase linearly with the scan rate from 10 to 100 mV/s. taking the first redox peak as a representative. The redox peak current has a good linear relationship with increasing scan rate, as indicated by the inset (Fig. 6), indicating that the electrode process is a surface-controlled process.

4.1. Detection of H_2O_2

Fig. 7 shows an amperometric response of the Ag NS modified GC electrode on successive injection of 1.0 mM H_2O_2 into the stirring (250 rpm) in an acetate buffer at an applied potential of −0.42 V. This modified GC electrode responded rapidly (9 s) when adding H_2O_2 into the stirring acetate buffer. The sensor could achieve the maximum steady-state current within 9 s with a detection limit of 1 μM (1.0×10^{-6} M) estimated at S/N – 3, which is lower than enzyme-based biosensors. The fast response should be attributed to the contribution of the good surface of Ag NSs attached on the GC electrode. From the calibration plot as shown in the left inset of Fig. 7, the sensor exhibits a linear response to the H_2O_2 concentration in the range of 0.25–1.4 μM (250–1400 mM). The reproducibility of the sensor was also investigated and the relative standard deviation (RSD) for H_2O_2 sensing was found to be less than 5% for five measurements for the same electrode.

The reproducibility and storage stability of the sensor was examined. When the Ag/GC modified electrode was stored in an air and subjected to the day-by-day calibrations at room temperature, the electrode can maintain over 95% of the initial value in the response to 2 mM H_2O_2 after 100 days, while the bulk Ag electrode decayed quickly to 90% after a day. Since the size of nanosilver synthesized and modified onto the GC electrode is larger than the bulk's diameter, the problem of catalyst leaking was minimized or eliminated. In addition, the nanosilver would be confined in a suitable matrix for the more catalytic stability and anti-contamination. Furthermore, we have tested the stability of adapted GC electrode (Ag/GC) and found that the reduction activity of H_2O_2 declined after 30 days. The transformed electrode stabilized for a longer time when compared with as prepared nanosilver without modification onto GC. The results confirmed that the Ag (0) nanosilver on the GC electrodes is steady while those outside the GC are fewer firm. As a consequence, they will not affect the stability of the sensor that uses the Ag (0) nanosilver catalysts confined onto the GC electrode and detection mechanism of H_2O_2 shown in the graphical abstract.

Table 1
Recovery experiment shows determination of H_2O_2 in tap water samples.

Real water samples	Added (μM)	Recovered (μM)	Percent recovery (%)
Tap water	1	0.92	92
	2	1.90	95
	3	2.98	99
	4	4.09	102
	5	5.27	105

4.2. Detection of H_2O_2 in tap water

To study the actual possibility of the proposed sensor, we checked the H_2O_2 sensor in true water samples. The tap water samples were obtained from the laboratory. The results of analysis obtained for tap water are presented in Table 1.

5. Conclusion

In this paper, we have demonstrated the application of green chemistry principles in the synthesis of nanosilver. FTIR confirms Azadirachtin as reducing and stabilizing agent for nanosilver formation. The particles produced are stable and comparable in size to those produced via physiochemical methods. The use of environmentally benign and renewable materials such as the neem kernel extract, offers numerous benefits ranging from environmental safety to ready integration of these nanomaterials to biologically relevant systems. This combination of solvent and renewable reactants presents a wide range of possibilities for the further development of green nanoparticles syntheses. The new application of the nanosilver confined onto the GC electrode is proposed. The uniform, high surface areas and tunable pore sizes onto the GC electrode facilitate its manipulation for sensor preparation and sensing application. The resulting nanosilver modified electrode shows very efficient electro catalytic behavior toward the reduction of H_2O_2 at a low over potential. The sensor for H_2O_2 exhibits very good analytical performance with low cost, convenient and sensitive and rapid detection. Thus, the Ag/GC is an attractive amperometric sensor for H_2O_2 and other analyte detection applications. This nanosilver may also be a promising candidate for electronics, systems, catalysis, fuel cells and nanodevices.

Acknowledgments

Authors are grateful to Department of Science and Technology and Council of Scientific and Industrial Research [CSIR-SRF (File No.-09/001/(0342)/2011/EMR-I)], Government of India for financial supports.

References

[1] Y. Sun, Y. Xia, Shape-controlled synthesis of gold and silver nanoparticles, Science 298 (2002) 2176–2179.
[2] B.R. Cuenya, Synthesis and catalytic properties of metal nanoparticles: size, shape, support, composition, and oxidation state effects, Thin Solid Films 518 (2010) 3127–3150.
[3] V.K. Shukla, R.P. Singh, A.C. Pandey, Black pepper assisted biomimetic synthesis of silver nanoparticles, J. Alloys Compd. 507 (2010) L13–L16.
[4] P.T. Anastas, J.C. Warner, Green Chemistry: Theory and Practice, Oxford University Press, New York, 1998.
[5] M. Poliakoff, P.T. Anastas, A principled stance, Nature 413 (2001) 257.
[6] A.S. Matlack, Introduction to Green Chemistry, Marcel Dekker, New York, 2001.

[7] J.M. Patete, X. Peng, C. Koenigsmann, Y. Xu, B. Karn, S.S. Wong, Viable methodologies for the synthesis of high-quality nanostructures, Green Chem. 13 (2011) 482–519.
[8] P.G. Jessop, Searching for green solvents, Green Chem. 13 (2011) 1391–1398.
[9] D. Mandal, M.E. Bolander, D. Mukhopadhyay, et al., The use of microorganisms for the formation of metal nanoparticles and their application, Appl. Microbiol. Biotechnol. 69 (2006) 485–492.
[10] A.R. Vilchis-Nestor, V. Sanchez-Mendieta, M.A. Camacho-Lopez, Solventless synthesis and optical properties of Au and Ag nanoparticles using *Camellia sinensis* extract, Mater. Lett. 62 (2008) 3103–3105.
[11] S.S. Shankar, A. Rai, B. Ankamwar, et al., Biological synthesis of triangular gold nanoprisms, Nat. Mater. 3 (2004) 482–488.
[12] J.L. Gardea-Torresdey, E. Gomez, J. Peralta-Videa, et al., Alfalfa sprouts: a natural source for the synthesis of silver nanoparticles, Langmuir 19 (2003) 1357–1361.
[13] N.H.H. Abu Bakar, J. Ismail, M. Abu Bakar, Synthesis and characterization of silver nanoparticles in natural rubber, Mater. Chem. Phys. 104 (2007) 276–283.
[14] N. Vigneshwaran, R.P. Nachane, R.H. Balasubramanya, et al., A novel one-pot 'green' synthesis of stable silver nanoparticles using soluble starch, Carbohydr. Res. 341 (2006) 2012–2018.
[15] S.P. Chandran, M. Chaudhary, R. Pasricha, et al., Synthesis of gold nanotriangles and silver nanoparticles using *Aloevera* plant extract, Biotechnol. Progr. 22 (2006) 577–583.
[16] S.S. Shankar, A. Rai, A. Ahmad, et al., Controlling the optical properties of lemongrass extract synthesized gold nanotriangles and potential application in infrared-absorbing optical coatings, Chem. Mater. 17 (2005) 566–572.
[17] V.K. Shukla, S. Pandey, A.C. Pandey, Green synthesis of silver nanoparticles using neem leaf (*Azadirachta indica*), Extract AIP Conf. Proc. 1276 (2010) 43–49.
[18] S.S. Shankar, A. Rai, A. Ahmad, M. Sastry, Rapid synthesis of Au, Ag, and bimetallic Au core–Ag shell nanoparticles using Neem (*Azadirachta indica*) leaf broth, J. Colloid Interface Sci. 275 (2004) 496–502.
[19] A.C. Templeton, S. Chen, S.M. Cross, R.W. Murray, Water-soluble, isolable gold clusters protected by tiopronin and coenzyme A monolayers, Langmuir 15 (1999) 66–76.
[20] P. Mulvaney, Surface plasmon spectroscopy of nanosized metal particles, Langmuir 12 (1996) 788–800.
[21] A. Ahmad, P. Mukherjee, S. Senapati, Extracellular biosynthesis of silver nanoparticles using the fungus *Fusarium oxysporum*, Colloids Surf. Biointerfaces B 28 (2003) 313–318.
[22] K. Cui, Y.H. Song, Y. Yao, Z.Z. Huang, L. Wang, A novel hydrogen peroxide sensor based on Ag nanoparticles electrodeposited on DNA-networks modified glassy carbon electrode, Electrochem. Commun. 10 (2008) 663–667.